

1 **Title:** Bluegill sunfish use high power-outputs from axial muscles to generate powerful suction-
2 feeding strikes

3

4 **Running Title:** Muscle power for suction feeding

5

6 **Authors:** Ariel L. Camp*†, Thomas J. Roberts, Elizabeth L. Brainerd

7

8 **Author Affiliations:**

9 Dept. of Ecology and Evolutionary Biology, Brown University, Providence, RI USA

10 †Present address: Dept. of Musculoskeletal Biology, Institute of Ageing and Chronic
11 Disease, University of Liverpool, Liverpool, UK

12

13 **Contact Information for Corresponding Author:**

14 *Dept. of Musculoskeletal Biology, Institute of Ageing and Chronic Disease, University
15 of Liverpool, Liverpool, UK

16 Ariel_Camp@liverpool.ac.uk

17

18 **Keywords:** XROMM, fluoromicrometry, muscle work, muscle power, shortening velocity

19

20 **Word Count:** 6714

21

22 **Figures:** 8

23

24 **Tables:** 2

25

26 **Supplementary Materials:** 1 Figure, 1 Table, 2 Movies

27

28 **Summary Statement:** Although the sternohyoideus muscle shortens to generate small amounts
29 of power, bluegill sunfish require large regions of axial musculature—operating at or near
30 maximum power output—to power suction feeding.

31 **Abstract**

32

33 Suction-feeding fish rapidly expand the mouth cavity to generate high-velocity fluid flows that
34 accelerate food into the mouth. Such fast and forceful suction expansion poses a challenge, as
35 muscle power is limited by muscle mass and the muscles in fish heads are relatively small. The
36 largemouth bass powers expansion with its large body muscles, with negligible power produced
37 by the head muscles (including the sternohyoideus). However, bluegill sunfish—with powerful
38 strikes but different morphology and feeding behavior —may use a different balance of cranial
39 and axial musculature to power feeding and different power outputs from these muscles. We
40 estimated the power required for suction expansion in sunfish from measurements of intraoral
41 pressure and rate of volume change, and measured muscle length and velocity. Unlike
42 largemouth bass, the sternohyoideus did shorten to generate power, but it and other head muscles
43 were too small to contribute more than 5-10% of peak expansion power in sunfish. We found no
44 evidence of catapult-style power amplification. Instead, sunfish powered suction feeding by
45 generating high power outputs (up to 438 W kg^{-1}) from their axial muscles. These muscles
46 shortened across the cranial half of the body as in bass, but at faster speeds that may be nearer
47 the optimum for power production. Sunfish were able to generate strikes of the same absolute
48 power as bass, but with 30-40% of the axial muscle mass. Thus, species may use the body and
49 head muscles differently to meet the requirements of suction feeding, depending on their
50 morphology and behavior.

51 **Introduction**

52

53 Fish can capture food underwater by creating high-velocity fluid flows that rapidly suck nearby
54 food and water into the mouth. These suction flows are generated as a fish quickly expands its
55 mouth cavity, increasing volume and decreasing pressure in this space so that water—and ideally
56 prey—are accelerated inside (reviewed in (Day et al., 2015)). To suction feed successfully, ray-
57 finned fishes (Actinopterygii) rely on a highly kinetic cranial skeleton that allows the mouth
58 cavity to expand three-dimensionally (Alexander, 1967). Mouth cavity volume may be increased
59 through elevation of the neurocranium (dorsal expansion), depression of the lower jaw and hyoid
60 apparatus (ventral expansion), and abduction of the suspensorium and operculum (lateral
61 expansion) (Liem, 1967; Liem, 1978; Van Wassenbergh et al., 2005; Van Wassenbergh et al.,
62 2009a). Any combination of these expansion systems may be used during suction feeding, which
63 contributes to prey capture in most of the over 30,000 species of ray-finned fishes (reviewed in
64 (Lauder, 1985; Wainwright et al., 2015; Westneat, 2006)).

65

66 Expanding the mouth cavity during suction feeding requires not only a mobile skeleton, but also
67 considerable muscle power and work. Mechanical power is the product of force and velocity, or
68 in a fluid system like suction feeding, the product of the rate of volume change and the change in
69 pressure (e.g., (Marsh et al., 1992)). The simultaneous rapid increase in volume and large
70 decrease in pressure of the mouth cavity during suction expansion requires substantial power.
71 However, vertebrate muscles can only generate a limited amount of power. The power produced
72 by an actively shortening muscle depends on many factors, but its maximum capacity is
73 ultimately limited by its mass: larger muscles generate more power than smaller muscles, all else
74 being equal. Meeting the requirements of powerful feeding behaviors, therefore, may be
75 particularly challenging, as the muscles of the head region are generally much less massive than
76 those of the rest of the body.

77

78 Researchers have long recognized that head muscles are likely too small to generate all the
79 power required for suction expansion (Aerts et al., 1987; Alexander, 1970; Elshoud-Oldenhave,
80 1979), and that additional power may come from the body muscles: the epaxials and hypaxials
81 (Fig. 1A). The primary expansive muscles in the head region include three cranial muscles—

82 levator arcus palatini, levator operculi, and dilator opercula—and a hypobranchial muscle, the
83 sternohyoideus (hereafter referred to together as “cranial” muscles). All are oriented to generate
84 lateral and ventral expansion (Fig. 1A) and are electrically active during suction expansion
85 (reviewed in (Grubich, 2001; Lauder, 1985; Westneat, 2006)), although cranial muscle
86 shortening has been measured in only a few instances (Camp et al., 2015; Carroll and
87 Wainwright, 2006; Van Wassenbergh et al., 2007a). The epaxial muscles are often considered
88 part of the feeding apparatus, as they are the only muscles that can elevate the neurocranium and
89 are consistently active during suction feeding (Lauder, 1985). Hypaxial muscles are less well
90 studied, but are generally active during feeding and can contribute to suction expansion by
91 retracting the pectoral girdle, and in turn the hyoid apparatus (Camp and Brainerd, 2014; Van
92 Wassenbergh et al., 2007a). These massive, fast-fiberd body muscles have the potential to
93 generate substantial power, which can be directly applied to the feeding apparatus during suction
94 expansion.

95
96 Suction expansion has been shown to be powered almost exclusively by the axial muscles in one
97 fish species, the largemouth bass (Camp et al., 2015). Bass have a large mouth opening (gape)
98 and volume, fusiform body, and rely on a combination of suction and forward acceleration i.e.,
99 “ram”, to capture prey (Norton and Brainerd, 1993). In bass, large regions—extending just over
100 half the body—of the epaxials and hypaxials shortened during suction expansion (Camp and
101 Brainerd, 2014). Despite shortening more slowly than the predicted optimum velocity for power
102 production, this large mass of musculature was capable of generating far more than the total
103 power required for even the most powerful strikes (Camp et al., 2015). In contrast, the four
104 cranial muscles together could not have generated more than 5% of the power for most strikes,
105 due to their small mass. None of these muscles except the levator operculi even shortened during
106 peak expansion power; instead they functioned to transmit axial muscle power and control mouth
107 expansion kinematics.

108
109 However, it remains unknown how other fishes—particularly those with different feeding
110 behaviors and/or morphology than largemouth bass—use the cranial and axial muscles to power
111 suction expansion. Bluegill sunfish are another well-studied suction-feeding species that are
112 closely related to largemouth bass (Near et al., 2004), but differ morphologically and in their

113 feeding kinematics. Where bass rely on ram, large volume changes and modestly low pressures
114 in the buccal cavity (up to 20 kPa below ambient (Carroll and Wainwright, 2006)) to capture
115 prey, sunfish use primarily suction with relatively little ram (Norton and Brainerd, 1993), very
116 low buccal pressures (35-50 kPa below ambient (Higham et al., 2006a; Lauder, 1980)) and small,
117 moderately rapid volume changes (Higham et al., 2006b). These kinematics suggest sunfish
118 produce powerful strikes, and while it remains to be experimentally demonstrated, it is
119 reasonable to expect that the axial muscles generate much of that power as they do in bass. Not
120 only do sunfish have different feeding kinematics, but compared to the fusiform bass they also
121 have shorter, deeper and more laterally compressed bodies and a smaller gape (Fig. 1B) (Smith
122 et al., 2015; Werner, 1977).

123
124 These differences make bluegill sunfish an interesting model for examining how cranial and
125 axial muscles are used to power strikes in species that are behaviorally and morphologically
126 distinct from largemouth bass. Sunfish could use a different mass of musculature by recruiting a
127 larger or smaller region of the axial muscles for active shortening, and/or by generating positive
128 power from more cranial muscles (including the sternohyoideus). They could also generate
129 relatively more power per unit muscle than bass, for example, by shortening their muscles at a
130 speed closer to the predicted optimum for power production (Carroll et al., 2009). Alternatively,
131 sunfish may use elastic energy storage to amplify their muscle power: shortening muscles slowly
132 before the strike to load energy into an elastic element, and then releasing it much more rapidly
133 at a higher power. Such a “biological catapult” power amplification is typified by muscle
134 activation and shortening preceding skeletal motion, and has been hypothesized in a suction-
135 feeding cichlid fish (Aerts et al., 1987) and demonstrated in the axial muscles of pipefish and
136 seahorses (Van Wassenbergh et al., 2008; Van Wassenbergh et al., 2009b). Like bass, pipefish
137 also rely almost exclusively on the axial muscles to power suction feeding, but in this species
138 epaxial and hypaxial muscle power is amplified by loading energy into the long tendons that
139 connect these muscles to the feeding apparatus (Van Wassenbergh et al., 2014; Van
140 Wassenbergh et al., 2008). Power amplification cannot increase the total energy or work, so it
141 still requires enough musculature to produce the necessary work of suction feeding. Our goal
142 was to determine which of these strategies bluegill sunfish use to generate high-powered suction
143 feeding: recruiting a large region of axial muscles for shortening, generating positive power from

144 more cranial muscles, producing higher mass-specific power outputs from their cranial and/or
145 axial muscles, and catapult-style power amplification of cranial and/or axial muscles.

146

147 To test these possibilities, we measured muscle shortening and expansion power to determine the
148 roles of the cranial and axial muscles in powering suction feeding in bluegill sunfish. As the
149 cranial and axial muscles are all known to be active during suction expansion in bluegill sunfish
150 (Lauder and Lanyon, 1980; Lauder et al., 1986), we assumed that any muscle shortening was
151 active and indicated power production. Muscle length changes throughout the epaxials and
152 hypaxials were measured with fluoromicrometry, which uses biplanar X-ray video to measure
153 the change in distance between radio-opaque, intramuscular markers (Camp et al., 2016). These
154 X-ray videos were also combined with digital bone models to create accurate and precise skeletal
155 animations of sunfish suction feeding with X-ray Reconstruction of Moving Morphology
156 (XROMM) (Brainerd et al., 2010). From the XROMM animations, we measured the skeletal
157 kinematics of expansion, whole-muscle length changes of the four non-axial muscles, and
158 instantaneous volume changes of the buccal cavity (using a dynamic digital endocast (Camp et
159 al., 2015)). Buccal volume dynamics were combined with pressure measurements from an
160 intraoral pressure probe to estimate the power and work required for suction expansion.
161 Measurements of mass for each muscle were taken post-mortem and used to estimate mass-
162 specific power and work production. These data allowed us to 1) estimate how powerful sunfish
163 suction strikes are, 2) determine which cranial muscles and regions of the axial musculature
164 shorten to generate power during suction feeding, and 3) test whether pre-shortening and elastic
165 energy storage were used to amplify muscle power during suction expansion in bluegill sunfish.

166

167 **Materials and Methods**

168 Two bluegill sunfish (*Lepomis macrochirus*, Rafinesque 1819)—Bluegill 1 (standard length 170
169 mm, total mass 164 g) and Bluegill 3 (standard length 167 mm and total mass 162 g)—were line-
170 caught in Providence, RI, USA, under a scientific collecting permit from the Rhode Island
171 Department of Environmental Management. All experimental procedures were approved by the
172 Brown University Institutional Animal Care and Use Committee.

173

174 Each fish was anesthetized and surgically implanted with bone and muscle markers and a
175 cannula for a pressure probe. Implantation techniques followed previously reported methods
176 (Camp and Brainerd, 2014; Camp et al., 2015) and are described briefly here. One to four radio-
177 opaque markers (tantalum spheres, 0.5 mm diameter) were implanted in the neurocranium,
178 urohyal and the left-side cleithrum, operculum, suspensorium, lower jaw (dentary and articular),
179 maxilla, and premaxilla (Fig. 1A). At least one marker was also implanted in the soft tissue of
180 the esophagus to demarcate the back of the mouth cavity. Intramuscular markers (0.8 mm
181 diameter) were implanted along the length of the epaxials (four markers) and hypaxials (three
182 markers), within the muscle but close to the dorsal and ventral surfaces. An additional three
183 markers implanted more deeply in the epaxials (Fig. 2A), together with three of the superficial
184 epaxial markers, were used to define a dorso-ventral body plane. Lastly, a cannula to house the
185 pressure probe was implanted in the ethmo-frontal region following established methods (Norton
186 and Brainerd, 1993). Fish were given a pre-operative analgesic (Butorphanol) and a
187 postoperative antibiotic (enrofloxacin), and recovered fully within three days—with no signs of
188 stress or difficulty caused by any of the implants.

189

190 *Data Recording*

191 We filmed suction feeding strikes from each fish with high-speed biplanar X-ray video and
192 simultaneously recorded intraoral pressure (Camp and Brainerd, 2014; Camp et al., 2015). Fish
193 were trained to feed on live goldfish prey in narrow (7 x 25.5 x 103.5 cm) tanks, as this
194 minimized the volume of water the X-rays passed through and gave the best quality images.
195 Some individual bluegill were reluctant to feed on live prey, and non-elusive prey (pellets)
196 yielded only low-motivation strikes, as judged by the magnitude of subambient pressure. We
197 collected, trained, instrumented and recorded data from five individuals, but only two of these
198 individuals, Bluegills 1 and 3, fed on live prey. Therefore, we report data from just two
199 individuals here because the focus of this study is high-performance strikes. Raw data from the
200 other three bluegills feeding on pellets are potentially available for further study (by
201 communication with the authors). Metadata for all individuals, including number of strikes and
202 food types, are viewable on XMA Portal (available at xmaportal.org, under study identifier
203 BROWN48).

204

205 Approximately dorsoventral and lateral view X-ray videos were generated at 200 mA and 105
206 (dorsoventral view) or 65 (lateral view) kV with a custom-made biplanar system (Imaging
207 Systems and Services, Painesville, OH, USA), and recorded at 500 frames s⁻¹ with Phantom v10
208 high-speed cameras (Vision Research, Wayne, NJ, USA). Images were also recorded of standard
209 grids and a calibration object—two sheets of acrylic embedded with 32 steel markers—to
210 remove distortion introduced by the X-ray machines and calibrate the 3D space imaged by both
211 videos (Brainerd et al., 2010). Pressure was measured with a SPR-407 Mikro-tip pressure probe
212 (Millar Instruments, Houston, TX, USA) inserted through the cannula, so it just protruded into
213 the mouth cavity. Pressures were recorded at 1,000 Hz with PowerLab and LabChart 7.2.2 (AD
214 Instruments, Colorado Springs, CO, USA), and the probe was calibrated before each day of
215 filming. A single trigger started both X-ray video and pressure recording, and daily
216 synchronization tests measured the timing offset (if any) between the onset of pressure and video
217 recordings. A total of 11 recorded strikes (six from Bluegill 1, five from Bluegill 3) were
218 analyzed. The associated X-ray video, pressure, and CT data (see below) are deposited and
219 publicly available in the XMA Portal (available at xmaportal.org, under study identifier
220 BROWN48).

221

222 Computed tomography (CT) scans were taken of each fish post-mortem with a Bruker Skyscan
223 1173 at a resolution of 0.13 mm pixel⁻¹ and a slice thickness of 0.13 mm. From these scans,
224 polygonal mesh models of each bone and its markers were generated in Horos (v2.1.2; Horos
225 Project, horosproject.org), and edited in GeoMagic 2013 (Research Triangle Park, NC, USA).
226 The position of each bone marker was then measured relative to the 3D bone models in Maya
227 2016 (Autodesk, San Rafael, CA, USA) using custom scripts in the “XROMM Tools” package,
228 available at xromm.org.

229

230 *XROMM*

231 Skeletal kinematics were reconstructed with marker-based XROMM, using XMA Lab ((Knorlein
232 et al., 2016), software and instructions available at <https://bitbucket.org/xromm/xmalab>) and
233 custom Maya scripts (available at https://bitbucket.org/xromm/xromm_mayatools). In XMA Lab,
234 all markers were tracked in both X-ray videos to calculate their XYZ coordinates with a tracking
235 precision of 0.065 mm or better across all bones and both individuals, measured as the mean

236 standard deviation of intraosseous marker distances (Brainerd et al., 2010). To improve contrast
237 and ease of marker-tracking, X-ray videos were first filtered with an unsharp mask in Adobe
238 Photoshop (CC 2017, Adobe Systems). For bones with at least three markers, XYZ coordinates
239 were combined with marker positions relative to the 3D bone models to calculate rigid body
240 transformations, which were filtered at 60 Hz low-pass Butterworth filter in XMALab and
241 applied to the 3D bone models in Maya. The six epaxial markers of the body plane were treated
242 as belonging to a single bone, and used to calculate the rigid body transformations of a polygonal
243 mesh plane (Camp and Brainerd, 2014). Bones with only one or two markers were animated in
244 Maya with scientific rotoscoping: hand-aligning a bone model to match the images of that bone
245 in both X-ray views (Gatesy et al., 2010). Both techniques were used to create a single XROMM
246 animation of all marked bones during each suction feeding strike (Fig. 2A, Movie S1).

247

248 *Skeletal kinematics*

249 From these XROMM animations, six-degree-of-freedom motions of the neurocranium,
250 cleithrum, and urohyal were measured relative to the body plane. Motions of each bone were
251 measured with a joint coordinate system (JCS), which calculated the relative motion between
252 two anatomical coordinate systems (ACSs) placed at a joint, one attached to the body plane and
253 one attached to the bone (Camp and Brainerd, 2014). Each JCS measured skeletal kinematics as
254 a set of translations along, and Euler angle rotations about, X, Y, and Z axes, following the right-
255 hand rule and a ZYX order of rotation. For the neurocranium, the ACSs were placed at the
256 craniovertebral joint, with the Z-axis oriented mediolaterally, the X-axis rostrocaudally, and the
257 Y-axis orthogonal to both the X- and Z-axes (Fig. 3A). Thus, the X-axis described rostrocaudal
258 translation and long-axis rotation (roll), the Y-axis described dorsoventral translation and
259 mediolateral rotation (yaw), and the Z-axis described transverse translation and rotation in the
260 sagittal plane (cranial elevation/depression). The ACSs of the cleithrum and urohyal had the
261 same orientation, but were placed at the rostradorsal edge of the cleithrum (near the cleithrum-
262 supracleithrum joint) and at the rostrventral protuberance of the urohyal, respectively (Fig. 3A).

263

264 *Dynamic endocast and volume calculation*

265 Volume changes of the buccal cavity were measured from the XROMM animations using a
266 dynamic digital endocast, as described previously (Camp et al., 2015). Briefly, a polygonal mesh

267 endocast was built to fill the left side of the mouth cavity as defined by the animated bones (Fig.
268 2C), with the vertices of the polygonal endocast linked to skeletal landmarks so the endocast
269 deformed as the animated bones moved (Movie S2). The volume of this left-side endocast was
270 calculated at each frame using a custom Maya script written by S. Gatesy (adapted from
271 www.vfxoerflow.com), and doubled to give the volume of the whole buccal cavity, assuming
272 bilateral symmetry.

273

274 *Muscle length changes*

275 Axial muscle length changes were measured from the biplanar X-ray videos using
276 fluoromicrometry: measuring muscle length as the change in distance between intramuscular
277 markers (Camp et al., 2016). Muscle markers were tracked and the XYZ coordinates calculated
278 in XMALab; all further calculations were done in MATLAB (R2015a; The Mathworks, Natick,
279 MA, USA). Marker coordinates were filtered at 60 Hz (low-pass Butterworth filter), and the
280 distance between each pair of markers (i.e., length change) calculated to determine which regions
281 of the epaxial and hypaxial muscles consistently shortened during suction feeding. The
282 rostralmost region of each muscle was defined as the distance between the rostralmost muscle
283 marker and a bone marker at the muscle attachment site on the neurocranium or cleithrum.
284 Muscle shortening was measured for every region, and all regions that consistently shortened
285 were included in the whole-muscle length of each axial muscle (Fig. S1). Based on this, whole-
286 muscle length of the epaxials was the distance from the neurocranium to the caudal edge of the
287 first (spiny) dorsal fin (shaded region in Fig. 1A). Whole-muscle length of the hypaxial muscles
288 extended from the ventral tip of the cleithrum to the rostral edge of the anal fin (shaded region in
289 Fig. 1A). Note that these “whole-muscle” lengths only represent shortening across these
290 superficial regions of the axial muscles measured by fluoromicrometry. They may not
291 necessarily be representative of fiber length changes outside of the region of measurement.
292 Cranial muscle lengths were measured from the XROMM animations by calculating the distance
293 between each muscle’s bony attachment sites (Camp et al., 2015). For each muscle, virtual
294 markers were placed on the animated bone models at the attachment points of representative
295 fibers and the whole muscle length measured as the change in distance between these markers
296 (Fig. 2B). Muscle length was normalized to its mean initial length prior to the onset of the strike
297 (L_i). For each muscle, whole muscle velocity was calculated at each time step as the change in

298 muscle length divided by the change in time, and expressed in $L_i s^{-1}$, with shortening indicated
299 by positive velocities.

300

301 *Power and work calculations*

302 Following the methods of Camp et al. (Camp et al., 2015), instantaneous suction expansion
303 power was estimated in MATLAB as the product of the rate of volume change ($m^3 s^{-1}$) and
304 buccal cavity pressure (Pa). Buccal pressure was filtered (low-pass Butterworth, 60 Hz cutoff)
305 resampled from 1,000 Hz to 500 Hz to match the frequency of the volume data, and expressed
306 relative to the initial, ambient pressure prior to the strike. At each time step the current and
307 subsequent pressure values were averaged and multiplied by -1, so that the product of
308 subambient pressures and increasing volume rates resulted in positive power. The work of
309 suction expansion was calculated as the integral (via the trapezoidal method) of the power-time
310 curve for each strike.

311

312 These work and power estimates have two main sources of error. First, they neglect the
313 additional power and work required to overcome the drag and inertia of accelerating the feeding
314 apparatus (Van Wassenbergh et al., 2015) and the inertia of shortening muscle masses. This
315 omission is most likely to result in our values underestimating the actual work and power
316 required to expand the mouth. Based on inverse dynamic models of suction feeding, which
317 calculated the pressure-volume power as well as the power required to overcome drag and
318 inertia, we expect this underestimate to be less 5-10% (Aerts et al., 1987; Muller et al., 1982;
319 Van Wassenbergh et al., 2015). Second, our power estimates are based on a single measurement
320 of pressure, which does not capture the spatial variation of intraoral pressure (Muller et al.,
321 1982). A computational fluid dynamics (CFD) model of a bluegill sunfish performing a single,
322 low-power suction strike found that using a single pressure value (the mean pressure in the
323 buccal cavity) resulted in an overestimate of peak instantaneous suction power (4.5 instead of 3
324 mW) (Van Wassenbergh, 2015). However, it is unclear if this can be extrapolated to the higher-
325 power strikes used in this study, or how the assumptions of this CFD model—for example,
326 modelling the buccal cavity as a radially symmetric, expanding cone—may also influence peak
327 power calculations. Therefore, it is difficult to determine the likely magnitude or direction of
328 error resulting from the use of a single pressure measurement to estimate power in this study.

329

330 For each fish, the four cranial muscles (including the sternohyoideus) and two axial muscles
331 were dissected out post-mortem, unilaterally, and weighed on a digital scale. Only the regions of
332 the epaxials and hypaxials that consistently shortened during suction feeding (Fig. 1A, and see
333 “Muscle Length” section for detailed description) were included in the mass measurements.
334 Unilateral masses were doubled to calculate the bilateral mass of each muscle (Table 1).
335 Suction expansion power and work were divided by the total axial muscle mass involved in
336 shortening to estimate the axial mass-specific power and work output of each strike. Similarly,
337 the cranial mass-specific power and work outputs were estimated by dividing the power and
338 work of suction expansion by the total cranial muscle mass (the summed bilateral mass of all
339 four muscles).

340

341 **Results**

342 Measurements of buccal cavity volume change and pressure were used to estimate the power and
343 work required for suction feeding strikes. To determine the role of each cranial (including the
344 sternohyoideus) and axial muscle in generating that power and work, we measured muscle mass,
345 length, and instantaneous velocity. Muscles can only generate power by actively shortening. As
346 all cranial and axial muscles studied here are known to be active during suction feeding in
347 sunfish (Lauder and Lanyon, 1980), we used measurements of muscle shortening to infer which
348 cranial muscles and regions of axial muscles generated power during suction expansion. Both
349 individuals studied showed broadly similar patterns but variable magnitudes in their kinematics,
350 muscle shortening, and buccal cavity expansion, so we report individual means and standard
351 errors (N = 6 strikes for Bluegill 1; N = 5 for Bluegill 3) below and in Tables 2-3 and S1.

352

353 *Axial muscle function*

354 Large regions of the epaxial and hypaxial muscles shortened during suction feeding to elevate
355 the neurocranium and retract the pectoral girdle, respectively. Relative to the body plane, the
356 neurocranium elevated (positive Z-axis rotation) by a mean peak of $11.9 \pm 1.6^\circ$ in Bluegill 1 and
357 13.7 ± 2.1 in Bluegill 3, while rotations about the other axes were generally smaller and highly
358 variable (Fig. 3B; Table S1). The cleithrum retracted (negative Z-axis rotation) relative to the
359 body plane by a mean peak of $-7.1 \pm 0.7^\circ$ in Bluegill 1 and $-4.6 \pm 1.0^\circ$ in Bluegill 3, and showed

360 a tendency for small rotations about the other two axes (Fig. 3B). Neither bone had substantial
361 translations (Table S1). Neurocranium elevation and pectoral girdle retraction were the result of
362 epaxial and hypaxial (respectively) muscle shortening. In both muscles, shortening extended
363 over halfway down the body (shaded region in Fig. 1A; see also Fig. S1). Across this entire,
364 superficial muscle region where shortening was measured (defined as the whole-muscle length),
365 maximum longitudinal shortening of the epaxial muscle mass reached a mean of $3.9 \pm 0.5\%$
366 (Bluegill 1) and $4.4 \pm 0.5\%$ (Bluegill 3) of initial length and maximum hypaxial shortening
367 reached a mean of $6.8 \pm 0.6\%$ (Bluegill 1) and $5.5 \pm 0.9\%$ (Bluegill 3) of initial length (Fig. 4,
368 Table 1). Mean epaxial muscle shortening velocity during the period of peak power output (i.e.,
369 when expansion power was within 25% of its maximum) was $2.2 \pm 0.3 \text{ L}_i \text{ s}^{-1}$ (Bluegill 1) and 1.9
370 $\pm 0.5 \text{ L}_i \text{ s}^{-1}$ (Bluegill 3). For the hypaxials, mean shortening velocity during peak power was 3.4
371 $\pm 0.2 \text{ L}_i \text{ s}^{-1}$ (Bluegill 1) and $2.1 \pm 0.6 \text{ L}_i \text{ s}^{-1}$ (Bluegill 3).

372

373 *Cranial muscle function*

374 The largest of the head muscles examined in this study, the sternohyoideus, consistently
375 shortened and contributed to retraction and depression of the urohyal. Relative to the body plane,
376 the urohyal translated caudally (negative X-axis) and ventrally (negative Y-axis), with little
377 medio-lateral translation or rotation (Z-axis) of this mid-sagittal bone (Fig. 3C; Table S1). While
378 the sternohyoid is not the only muscle that can contribute to urohyal translation, sternohyoid
379 muscle shortening usually coincided with urohyal retraction (Fig. 5). Over its whole length, the
380 sternohyoideus shortened by a mean of $12 \pm 1\%$ in Bluegill 1 and $4.3 \pm 1.2\%$ in Bluegill 3 (Fig.
381 4, Table 1), and had a mean shortening velocity of $4.4 \pm 0.5 \text{ L}_i \text{ s}^{-1}$ (Bluegill 1) and $1.4 \pm 0.7 \text{ L}_i \text{ s}^{-1}$
382 (Bluegill 3) during peak power. Of the remaining cranial muscles, only the levator operculi
383 consistently shortened during peak expansion power, with a mean maximum strain of $6.9 \pm 1.1\%$
384 (Bluegill 1) and $7.3 \pm 0.9\%$ (Bluegill 3) and mean shortening velocity of $3.2 \pm 1.0 \text{ L}_i \text{ s}^{-1}$ (Bluegill
385 1) and $3.3 \pm 0.6 \text{ L}_i \text{ s}^{-1}$ (Bluegill 3) during peak power. The dilator operculi and the levator arcus
386 palatini muscles maintained a fairly constant length—or even lengthened—during peak
387 expansion power, and only started to shorten after peak expansion power occurred (Fig. 4).

388

389 *Suction expansion power and work*

390 The mouth expansion generated by these muscle strains and skeletal kinematics resulted in
391 subambient pressures and rapid volume changes in the buccal cavity, and generally required
392 substantial power. Subambient pressures varied across strikes, with peak values from -12 to -38
393 kPa, while the rate of mouth volume change reached a mean maximum of $387 (\pm 58) \text{ cm}^3 \text{ s}^{-1}$ in
394 Bluegill 1 and $351 (\pm 75) \text{ cm}^3 \text{ s}^{-1}$ in Bluegill 3 (Table 2). Peak expansion power occurred about 5-
395 10 ms before peak gape (Fig. 5, Table 2). The magnitude of peak power ranged from 0.55 to 18
396 W across all measured strikes (Fig. 6). When expressed as power per unit axial (i.e., summed
397 hypaxial and epaxial) muscle mass, the resulting mass-specific peak powers ranged from 14 to
398 438 W kg^{-1} (mean $277 \pm 51 \text{ W kg}^{-1}$ for Bluegill 1 and $133 \pm 54 \text{ W kg}^{-1}$ for Bluegill 3) (Fig. 6).
399 When the peak expansion powers were expressed as power per unit cranial (including the
400 sternohyoideus) muscle mass, mass-specific powers ranged from 192 to $9,691 \text{ W kg}^{-1}$ (mean
401 $6,126 \pm 1,127 \text{ W kg}^{-1}$ for Bluegill 1 and $1,832 \pm 740 \text{ W kg}^{-1}$ for Bluegill 3) (Fig. 6).

402

403 The work required for each mouth expansion event was estimated as the area under the power-
404 time curve, and expressed per unit axial muscle mass and per unit cranial muscle mass (Figs. 7-
405 8). The axial mass-specific expansion work had a range of 0.24 to 5.6 J kg^{-1} (Fig. 8B) and a
406 mean of $3.3 \pm 0.7 \text{ J kg}^{-1}$ for Bluegill 1 and $1.9 \pm 0.6 \text{ J kg}^{-1}$ for Bluegill 3 (Table 2). Cranial mass-
407 specific expansion work ranged from 3.4 to 124 J kg^{-1} , with a mean of $73 (\pm 14.6) \text{ J kg}^{-1}$ for
408 Bluegill 1 and $26.1 (\pm 8.5) \text{ J kg}^{-1}$ for Bluegill 3 (Table 2). For comparison, we also calculated the
409 absolute and axial mass-specific expansion work of largemouth bass using previously collected
410 data (Camp et al., 2015). The absolute expansion work ranged from 0.015 to 0.48 J across all
411 recorded strikes from the three bass (Fig. 8A). Mean axial mass-specific work was $0.36 (\pm 0.08)$,
412 $2.5 (\pm 0.4)$, and $0.85 (\pm 0.01)$ for Bass 1 ($n = 10$ strikes), Bass2 ($n = 9$ strikes) and Bass3 ($n=10$
413 strikes), respectively (Fig. 8B).

414

415 **Discussion**

416 Bluegill sunfish generated large subambient pressures and rapid volume changes in the buccal
417 cavity to produce powerful strikes. Buccal pressures were similar to those reported previously
418 (Carroll and Wainwright, 2009; Higham et al., 2006a) and the mean peak rate of volume change
419 was about 1.5 times more than previously reported for similarly-sized sunfish (Higham et al.,
420 2006b). Of the four head muscles examined, the sternohyoideus and levator operculi muscles

421 consistently shortened during peak expansion power. However, these muscles were too small to
422 directly generate meaningful amounts of power, and we found no evidence of power
423 amplification through elastic energy storage in these or any other muscle. Instead, sunfish relied
424 on high power outputs from their axial muscles. These muscles shortened across the same region
425 as largemouth bass—from the head to over halfway down the body (Camp and Brainerd,
426 2014)—but with substantially higher estimated muscle mass-specific power outputs of up to 300-
427 438 W kg⁻¹ (Fig. 6). Both species generated absolute peak expansion powers of 10-15 W during
428 suction feeding (Fig. 6, (Camp et al., 2015)), but the sunfish in this study produced these strikes
429 with less than half the axial muscle mass of the larger bass individuals from our prior study
430 (Camp et al., 2015). Sunfish axial muscles also shortened at faster velocities than those of bass
431 and may have been nearer the optimum for power production (Carroll et al., 2009), which likely
432 contributed to the higher power output of these muscles. We conclude that bluegill sunfish rely
433 on high power outputs from the axial muscles to generate fast and forceful suction feeding
434 strikes.

435

436 *Cranial muscle function*

437 In bluegill sunfish, two cranial muscles—the sternohyoideus and levator operculi—consistently
438 shortened during peak expansion power (Fig. 4). Although muscle power was not measured
439 directly, we infer that muscle shortening indicates power production because these muscles are
440 known to be active during suction expansion (Lauder and Lanyon, 1980; Lauder et al., 1986).
441 Additionally, the skeletal motions produced by these shortening muscles occur against inertial
442 and hydrodynamic resistance and therefore require power. The levator operculi shortened by
443 about 7% in both individuals, presumably elevating (i.e., dorsally rotating in a parasagittal plane)
444 the operculum. This motion may not directly expand the mouth, but can be transmitted through
445 the opercular linkage, a set of bones and ligaments, to contribute to lower jaw depression
446 (Ballintijn, 1969; Liem, 1980). In largemouth bass, the levator operculi's shortening holds the
447 operculum in place relative to the body—against resistance from the suspensorium—and allows
448 epaxial-powered neurocranium elevation to be transmitted through this linkage to the lower jaw
449 (Camp and Brainerd, 2015). Thus, even when cranial muscles are generating power, they can
450 still function to transmit axial muscle power. As in largemouth bass, the levator operculi
451 shortened relatively quickly and reached a mean peak velocity of about 3 lengths (L_i) s⁻¹, which

452 actually exceeds the optimum velocities for power production (~ 1.6 muscle lengths s^{-1})
453 calculated for the sternohyoideus muscle of sunfish (Carroll et al., 2009). The levator operculi of
454 bluegill sunfish may have a similar role to that of bass during suction feeding (Camp and
455 Brainerd, 2015), but further study of the opercular kinematics is needed to confirm this.

456
457 The sternohyoideus muscle shortened to retract the urohyal and hyoid apparatus (Fig. 5E), as
458 predicted by Lauder and Lanyon (Lauder and Lanyon, 1980). However, in contrast to these
459 authors' hypothesized function, the hypaxial muscles also shortened at the same time to retract
460 the cleithrum (Fig. 5D). As these muscles are in series (Fig. 1A) and both active during suction
461 feeding, it was proposed that the hypaxials produce only force to hold the pectoral girdle
462 immobile and provide a stable attachment site for the sternohyoideus to shorten against (Lauder
463 and Lanyon, 1980). In largemouth bass and clariid catfishes, the only other species where both
464 muscle lengths have been measured, the opposite occurred: the hypaxials shortened while the
465 sternohyoideus maintained a relatively constant length or was stretched as it transmitted hypaxial
466 power to the hyoid (Camp and Brainerd, 2014; Van Wassenbergh et al., 2005; Van Wassenbergh
467 et al., 2007b). Our data from bluegill sunfish are the first empirical evidence of both muscles
468 shortening during peak expansion power to generate positive power for hyoid retraction and
469 depression. The sternohyoideus muscle in Bluegill 1 shortened relatively quickly, with mean
470 peak velocities of about $4 L_i s^{-1}$, exceeding the optimum velocity for power production (~ 1.6
471 muscle lengths s^{-1}) calculated for this muscle in similarly sized sunfish (Carroll et al., 2009),
472 although in Bluegill 3 it shortened more slowly ($1.4 L_i s^{-1}$).

473 474 *Cranial muscle power and work*

475 While the sternohyoideus and levator operculi did shorten during peak expansion power, the
476 power output from these small muscles would have been negligible compared to that required for
477 most suction strikes. These and the other cranial muscles together would have needed power
478 outputs of up to $9,691 W kg^{-1}$ to directly power suction expansion by themselves (Fig. 6), which
479 far exceeds the maximum recorded from or any vertebrate muscle ($1,121 W kg^{-1}$ (Askew and
480 Marsh, 2001)). Even assuming the relatively high muscle mass-specific power output of $438 W$
481 kg^{-1} inferred for the axial muscles, the sternohyoideus muscle could not have generated more
482 than $1 W$ of power or 5-10% of the peak power required for the most powerful strikes. Put

483 another way, including the sternohyoideus muscle mass—by far the largest of the four cranial
484 muscles examined—with the axial muscles would only lower the maximum power output
485 estimated for the axial muscles from 438 to 422 W kg⁻¹. The muscles of the head likely make
486 important contributions to suction feeding kinematics (see above), but are not a major source of
487 direct muscle power for bluegill sunfish.

488

489 Additionally, we found no evidence that the bluegill sunfish's cranial muscle power was
490 amplified by elastic energy storage prior to suction expansion. Such power amplification
491 mechanisms are usually associated with muscle shortening and activation prior to skeletal motion
492 (Astley and Roberts, 2012; Van Wassenbergh et al., 2008), but we did not observe any muscle
493 shortening prior to suction expansion in sunfish (Fig. 4, Table 1), even during the most powerful
494 strike (Fig. 5), nor have the cranial muscles been reported to activate prior to suction expansion
495 in bluegill sunfish (Lauder and Lanyon, 1980; Lauder et al., 1986). Moreover, such elastic
496 energy storage would still require the cranial muscles to generate the work for suction expansion.
497 We estimated that the cranial muscles have the potential to generate about 25 J kg⁻¹ of work
498 under the conditions observed in suction feeding (Fig. 7A), but most suction strikes would have
499 required at least 40-60 J kg⁻¹ of work from these muscles (Fig. 7B). These work estimates follow
500 the work capacity calculations of Peplowski and Marsh (Peplowski and Marsh, 1997), and
501 assume a maximum isometric muscle stress of 30 N cm⁻², a 50% decrease in force due to force-
502 velocity effects during rapid shortening, and that the muscles shorten by 15% of their initial
503 length (the maximum shortening measured in this study (Fig. 4)). The small mass of the cranial
504 muscles in bluegill sunfish limits the work and power they can contribute to suction feeding
505 strikes.

506

507 *Axial muscle power and work*

508 As the cranial muscles could generate relatively little power or work, we conclude that bluegill
509 sunfish relied almost exclusively on the large axial muscles to generate powerful suction feeding
510 strikes. Despite their different (i.e., shorter and deeper) body shape, sunfish shortened epaxial
511 and hypaxial muscles over the same region as bass: from the muscles' cranial attachment sites on
512 the neurocranium and pectoral girdle to the caudal edge of the first dorsal fin and the rostral edge
513 of the anal fin, respectively (Fig. 1A). It is interesting that the magnitude of shortening was not

514 distributed evenly across the axial muscle of sunfish (Fig. S1), as in bass (Camp and Brainerd,
515 2014), but the functional implications of this remain unclear. Muscle activity has only been
516 measured and confirmed via electromyography in the most rostral portion of these muscles
517 during suction feeding in sunfish (Lauder and Lanyon, 1980), but we presume these regions
518 actively shortened. Axial muscle shortening contributes directly to dorsoventral expansion of the
519 buccal cavity by elevating the neurocranium and retracting the pectoral girdle (Fig. 3) against
520 suction pressure and inertial forces (Van Wassenbergh et al., 2015). These skeletal motions also
521 allow axial muscle power to be transmitted to the rest of the skull, via musculoskeletal linkages,
522 to generate the full, three-dimensional expansion of the buccal cavity. These results further
523 emphasize the role hypaxial muscles and pectoral girdle retraction can play in powering suction
524 feeding and expanding the mouth cavity. While the potential for contribution of epaxial muscles
525 to suction feeding has been recognized (e.g., (Carroll and Wainwright, 2009; Lauder and
526 Lanyon, 1980), the role of hypaxial muscles has received less attention (e.g., (Carroll and
527 Wainwright, 2009)).

528
529 Bluegill sunfish relied on high power-outputs from their axial muscles—rather than recruiting a
530 larger region of axial muscles or generating power from more cranial muscles—to meet the
531 mechanical demands of suction feeding. The sunfish in this study generated similar absolute
532 peak expansion powers (up to 18 W) as the largemouth bass (up to 15 W) from our previous
533 study, even though the sunfish were shorter (standard length of ~170 mm compared to ~300 mm
534 for bass) and had a total mass of shortening axial muscle only 30-40% of the axial muscle mass
535 of bass (Table 2, (Camp et al., 2015)). Therefore, the most powerful bass strike needed only 141
536 W kg^{-1} of axial muscle power output (Camp et al., 2015), while the axial muscle of sunfish was
537 estimated to generate 438 W kg^{-1} for most powerful strike (Fig. 6). High instantaneous power
538 outputs are not unexpected for these white-, fast-fibered muscles, which fish also use for
539 powerful escape behaviors, i.e., C-starts (Frith and Blake, 1995; Rome et al., 1988). Even the
540 highest muscle power output estimated here (438 W kg^{-1}) is within the maximum measured from
541 fish axial muscle with *in vitro* work loops (Altringham et al., 1993) and other vertebrate muscles
542 (Askew and Marsh, 2001; Curtin et al., 2005). As it is unlikely that we captured the maximum
543 suction feeding performance of bluegill sunfish, especially given our relatively small sample size
544 (e.g., (Astley et al., 2013)), the maximum power outputs of these muscles could be even higher.

545 However, our axial mass-specific power outputs should be interpreted with some caution, as they
546 are based on expansion power estimates with their own sources of error (see Materials and
547 Methods), and not direct measurements of muscle power production. For most strikes, our
548 estimated axial muscle mass-specific power outputs are at or below the maximum power output
549 of 300 W kg^{-1} (Fig. 6) previously estimated for bluegill sunfish (Carroll and Wainwright, 2009).

550

551 The shortening velocities measured from the axial muscles are consistent with these muscles
552 operating at or near their maximum power production. The epaxials and hypaxials shortened at
553 2-3 initial lengths (L_i) s^{-1} during peak expansion power (Table 1), approaching the optimum
554 velocity (V_{opt}) of power production of 3.3 or 4 $L_i s^{-1}$ for “myotomal” and epaxial muscle (Fig.
555 4B), respectively, of similarly sized bluegill sunfish (Carroll et al., 2009). The axial muscles of
556 largemouth bass shortened much more slowly ($0.5\text{-}1.6 L_i s^{-1}$), both compared to sunfish and to
557 the V_{opt} of 4 $L_i s^{-1}$ measured for this species (Carroll et al., 2009; Coughlin and Carroll, 2006).
558 We hypothesize that sunfish may achieve higher mass-specific power outputs from their axial
559 muscles, compared to bass, by shortening these muscles at speeds near the optimum for power
560 production. However, shortening velocity is just one component of muscle power, and
561 measurements of muscle activation, force production, and fiber length dynamics are need are
562 needed to better understand power production in these muscles.

563

564 Additionally, our measurements of longitudinal axial muscle shortening velocity may not be
565 representative of fiber-level strains across the entire volume of the hypaxials and epaxials. Whole
566 muscle velocity was measured across superficial regions near the midsagittal plane. In reality,
567 the magnitude and velocity of shortening may vary throughout these muscles as a result of the
568 complex fiber orientation of the axial muscles (Alexander, 1969; Gemballa and Vogel, 2002),
569 and/or the distance from the neutral axis of cranial/pectoral rotation. For example, during
570 swimming the muscle fibers furthest from the neutral axis of bending (i.e., the vertebral column)
571 would be expected to shorten more quickly than those closest to the neutral axis, if the body
572 bends like a simple homogenous beam (Shadwick et al., 1998), and yet muscle fiber orientations
573 act to homogenize fiber-level strain during swimming (Azizi and Brainerd, 2007; Rome and
574 Sosnicki, 1991). While our velocity measurements may therefore not be representative of the
575 entire muscle, the high powers measured for the entire musculature (near or even above their

576 measured maximum of 300 W kg^{-1} (Carroll et al., 2009)) would seem to support the idea that
577 fibers throughout the axial muscles are shortening at velocities near optimal for power
578 production.

579
580 It is also possible that some kind of elastic energy storage mechanism is used to amplify axial
581 muscle power, particularly during the most powerful strikes. The estimated work of suction
582 expansion was well within the expected work capacity of the axial muscles: requiring outputs of
583 no more than 6 J kg^{-1} (Figs. 7-8), so these muscles could be using mechanisms to amplify the rate
584 of energy production, i.e., power. While we found no evidence of catapult-style power
585 amplification (such as active muscle shortening prior to suction expansion and axial muscles
586 with long tendons, as in pipefishes (Van Wassenbergh et al., 2014; Van Wassenbergh et al.,
587 2008)), it is possible these muscles may be using a subtler mechanism. For example, energy
588 generated at the beginning of shortening could be stored in connective tissues or myoseptal
589 tendons and then released later in the contraction to amplify peak power. However, further
590 measurements of axial fiber activation and lengths—rather than the whole-muscle lengths
591 recorded here—and force outputs are needed to test this.

592
593 In contrast to the high mass-specific muscle power-output (Fig. 6), the mechanical work required
594 for these bluegill sunfish strikes was more similar to that of the largemouth bass from our
595 previous study (Fig. 8). The absolute work of suction expansion—the product of pressure and
596 volume or the integral of the power-time curve—in sunfish strikes was similar or less than that of
597 bass (Fig. 8A). The maximum work recorded from a sunfish strike (0.25 J) was about half the
598 maximum observed in the bass (0.50 J), although there was considerable overlap in the range of
599 expansion work for both species (Fig. 8A). As the absolute peak expansion power was similar
600 between sunfish and bass, this difference in expansion work may reflect a greater duration of
601 suction expansion in bass. For example, in the sunfish strike shown in Fig. 5, positive power is
602 generated over about 30 ms, while in the bass strike shown in Fig. 3 of (Camp et al., 2015)
603 positive power occurs over about 60 ms. The bluegill sunfish strikes measured in this study had
604 similar or slightly higher mass-specific work outputs for the axial muscles than those of the
605 largemouth bass measured previously (Fig. 8B): average axial mass-specific work was $0.36\text{-}2.5 \text{ J}$
606 (depending on individual) in largemouth bass compared to 1.8 and 3.4 J in Bluegill 1 and 3,

607 respectively (Fig. 7, Table 2). Thus, the axial muscles of sunfish had to generate only somewhat
608 higher work outputs, but much higher power outputs than bass to generate suction expansion.
609 Conversely, the slower axial muscle shortening velocities measured in bass may be related to
610 slower mouth expansion, and the need for these muscles to generate work but not particularly
611 high power-outputs.

612

613 *Concluding remarks*

614 Our results show that bluegill sunfish rely on high power outputs from their axial muscles to
615 meet the challenge of powerful feeding as a small-mouthed, deep-bodied, suction-reliant species.
616 Largemouth bass strikes also required power from the axial muscles, but in sunfish large regions
617 of axial musculature had to operate at or near maximum power output to produce the most
618 powerful suction strikes observed. While this supports the presence of axial-powered feeding in a
619 broader range of fishes beyond those with bass-like body shapes, it also highlights how the use
620 of axial power may vary with body shape as well as feeding behavior. Together with previous
621 studies, these results demonstrate that we must take feeding functions into account in order to
622 understand the morphology, physiology, and evolution of these body muscles in fishes. While
623 the axial muscles can generate the power for suction expansion, it is the cranial muscles and
624 skeleton that generate the three-dimensional motion and anterior-to-posterior progression of
625 suction expansion. These functions are no less important than power generation, and may be
626 achieved with or without muscle shortening during peak expansion power. For example, the
627 sternohyoideus muscle shortens to generate power in bluegill sunfish, but maintains a constant
628 length in bass to transmit hypaxial muscle power. A major challenge remains to understand how
629 the muscles of the head, together with the complex cranial skeleton, transmit axial muscle power
630 and control suction feeding kinematics.

631

632 **Acknowledgements**

633 We are grateful to the many members of the Brown EEB Morphology Group whose assistance
634 made this work possible, including E. Giblin, J. Lomax, J. Laurence-Chasen, and N. Chen (fish
635 surgery and X-ray filming); D. Sleboda, P. Feltman, and K. Rivard (specimen collection); S.
636 Gatesy (dynamic digital endocast method); R. Kambic (skeletal animation techniques). We also

637 appreciate the CT scanning facilities provided by the Karl F. Liem Bioimaging Center at Friday
638 Harbor Laboratories, University of Washington.

639

640 **Competing Interests**

641 No competing interests declared.

642

643 **Funding**

644 This work was supported by the National Science Foundation [IOS-1655756
645 to E.B. and A.C., DBI-1661129 to E.B., and IOS-1354289 to T. R.], a Brown University EEB
646 Doctoral Dissertation Development Grant [A.C.], and the Bushnell Graduate Research and
647 Education Fund [A.C.].

648

649 **Data Availability**

650 Data are available on the XMA Portal (xmaportal.org) in the study “Sunfish suction feeding”,
651 with the identifier BROWN48.

652

653 **Author Contributions**

654 Conceptualization, A.L.C., E.L.B., T.J.R.; Investigation, A.L.C.; Formal Analysis, A.L.C.,
655 E.L.B., T.J.R.; Writing, A.L.C.; Review & Editing, A.L.C., E.L.B., T.J.R.; Visualization, A.L.C.;
656 Supervision, E.L.B., T.J.R.

657

658 **List of Abbreviations**

659	ACS	Anatomical coordinate system
660	CFD	Computational fluid dynamics
661	CT	Computed tomography
662	DO	Dilator operculi
663	JCS	Joint coordinate system
664	L_i	Initial muscle length
665	LAP	Levator arcus palatini
666	LO	Levator operculi
667	SH	Sternohyoideus

668 V_{opt} Optimal muscle shortening velocity for power production
669 XROMM X-ray reconstruction of moving morphology

670

671 **References**

672

673 Aerts, P., Osse, J., Verraes, W., 1987. Model of jaw depression during feeding in *Astatotilapia*
674 *elegans* (Teleostei: Cichlidae): Mechanisms for energy storage and triggering. *J Morphol*
675 194, 85-109.

676 Alexander, R., 1967. Feeding. In: Cain, A. J., (Ed.), *Functional Design in Fishes*. Hutchinson and
677 Co, London.

678 Alexander, R., 1970. Mechanics of the feeding action of various teleost fishes. *J. Zool., Lond*
679 162, 142-156.

680 Alexander, R. M., 1969. The orientation of muscle fibres in the myomeres of fishes. *J Mar Biol*
681 *Assoc UK* 49, 263-290.

682 Altringham, J. D., Wardle, C. S., Smith, C. I., 1993. Myotomal muscle function at different
683 locations in the body of a swimming fish. *J Exp Biol* 182, 191-206.

684 Askew, G. N., Marsh, R. L., 2001. The mechanical power output of the pectoralis muscle of
685 blue-breasted quail (*Coturnix chinensis*): the in vivo length cycle and its implications for
686 muscle performance. *J Exp Biol* 204, 3587-3600.

687 Astley, H. C., Roberts, T. J., 2012. Evidence for a vertebrate catapult: elastic energy storage in
688 the plantaris tendon during frog jumping. *Biol Lett* 8, 386-389.

689 Astley, H. C., Abbott, E. M., Azizi, E., Marsh, R. L., Roberts, T. J., 2013. Chasing maximal
690 performance: a cautionary tale from the celebrated jumping frogs of Calaveras County. *J*
691 *Exp Biol* 216, 3947-53, doi:10.1242/jeb.090357.

692 Azizi, E., Brainerd, E. L., 2007. Architectural gear ratio and muscle fiber strain homogeneity in
693 segmented musculature. *J Exp Zool A Ecol Genet Physiol* 307, 145-55,
694 doi:10.1002/jez.a.358.

695 Ballintijn, C., 1969. Functional anatomy and movement co-ordination of the respiratory pump of
696 the carp (*Cyprinus carpio* L.). *J Exp Biol* 50, 547-567.

697 Brainerd, E. L., Baier, D. B., Gatesy, S. M., Hedrick, T. L., Metzger, K. A., Gilbert, S. L.,
698 Crisco, J. J., 2010. X-ray reconstruction of moving morphology (XROMM): precision,
699 accuracy and applications in comparative biomechanics research. *J Exp Zool* 313A, 262-
700 279, doi:10.1002/jez.589.

701 Camp, A. L., Brainerd, E. L., 2014. Role of axial muscles in powering mouth expansion during
702 suction feeding in largemouth bass (*Micropterus salmoides*). *J Exp Biol* 217, 1333-1345,
703 doi:Doi 10.1242/Jeb.095810.

704 Camp, A. L., Brainerd, E. L., 2015. Reevaluating Musculoskeletal Linkages in Suction-Feeding
705 Fishes with X-Ray Reconstruction of Moving Morphology (XROMM). *Integr Comp Biol*
706 55, 36-47, doi:10.1093/icb/icv034.

707 Camp, A. L., Roberts, T. J., Brainerd, E. L., 2015. Swimming muscles power suction feeding in
708 largemouth bass. *Proc Natl Acad Sci U S A* 112, 8690-5, doi:10.1073/pnas.1508055112.

709 Camp, A. L., Astley, H. C., Horner, A. M., Roberts, T. J., Brainerd, E. L., 2016.

710 Fluoromicrometry: a method for measuring muscle length dynamics with biplanar

711 videofluoroscopy. *Journal of Experimental Zoology, Part A* 325A, 399-408,
712 doi:10.1002/jez.2031.

713 Carroll, A. M., Wainwright, P. C., 2006. Muscle function and power output during suction
714 feeding in largemouth bass, *Micropterus salmoides*. *Comp Biochem Physiol A Mol*
715 *Integr Physiol* 143, 389-99, doi:10.1016/j.cbpa.2005.12.022.

716 Carroll, A. M., Wainwright, P. C., 2009. Energetic limitations on suction feeding performance in
717 centrarchid fishes. *J Exp Biol* 212, 3241-51, doi:10.1242/jeb.033092.

718 Carroll, A. M., Ambrose, A. M., Anderson, T. A., Coughlin, D. J., 2009. Feeding muscles scale
719 differently from swimming muscles in sunfish (Centrarchidae). *Biol Lett* 5, 274-7,
720 doi:10.1098/rsbl.2008.0647.

721 Coughlin, D. J., Carroll, A. M., 2006. In vitro estimates of power output by epaxial muscle
722 during feeding in largemouth bass. *Comp Biochem Physiol A Mol Integr Physiol* 145,
723 533-9, doi:10.1016/j.cbpa.2006.08.026.

724 Curtin, N., Woledge, R., Aerts, P., 2005. Muscle directly meets the vast power demands in agile
725 lizards. *P Roy Soc B-Biol Sci* 272, 581-584.

726 Day, S. W., Higham, T. E., Holzman, R., Van Wassenbergh, S., 2015. Morphology, Kinematics,
727 and Dynamics: The Mechanics of Suction Feeding in Fishes. *Integr Comp Biol* 55, 21-35,
728 doi:10.1093/icb/icv032.

729 Elshoud-Oldenhave, M. J. W., 1979. Prey capture in the Pike-Perch, *Stizostedion lucioperca*
730 (Teleostei, Percidae) structural and functional analysis. *Zoomorphologie* 93, 1-32.

731 Frith, H., Blake, R., 1995. The mechanical power output and hydromechanical efficiency of
732 northern pike (*Esox lucius*) fast-starts. *The Journal of Experimental Biology* 198, 1863.

733 Gatesy, S. M., Baier, D. B., Jenkins, F. A., Dial, K. P., 2010. Scientific rotoscoping: a
734 morphology-based method of 3-D motion analysis and visualization. *J Exp Zool* 313,
735 244-261, doi:10.1002/jez.588.

736 Gemballa, S., Vogel, F., 2002. Spatial arrangement of white muscle fibers and myoseptal
737 tendons in fishes. *Comp Biochem Physiol A Mol Integr Physiol* 133, 1013-1037.

738 Grubich, J. R., 2001. Prey capture in actinopterygian fishes: a review of suction feeding motor
739 patterns with new evidence from an elopomorph fish, *Megalops atlanticus*. *Am Zool* 41,
740 1258-1265.

741 Higham, T. E., Day, S. W., Wainwright, P. C., 2006a. The pressures of suction feeding: the
742 relation between buccal pressure and induced fluid speed in centrarchid fishes. *J Exp Biol*
743 209, 3281-7, doi:10.1242/jeb.02383.

744 Higham, T. E., Day, S. W., Wainwright, P. C., 2006b. Multidimensional analysis of suction
745 feeding performance in fishes: fluid speed, acceleration, strike accuracy and the ingested
746 volume of water. *J Exp Biol* 209, 2713-25, doi:10.1242/jeb.02315.

747 Lauder, G., 1980. The suction feeding mechanism in sunfishes (*Lepomis*) - An experimental
748 analysis. *J Exp Biol* 88, 49-72.

749 Lauder, G., Lanyon, L., 1980. Functional anatomy of feeding in the bluegill sunfish, *Lepomis*
750 *macrochirus*: in vivo measurement of bone strain. *J Exp Biol* 84, 33-55.

751 Lauder, G., Wainwright, P., Findeis, E., 1986. Physiological mechanisms of aquatic prey capture
752 in sunfishes: functional determinants of buccal pressure changes. *Comparative*
753 *Biochemistry and Physiology Part A: Physiology* 84, 729-734.

754 Lauder, G. V., 1985. Aquatic feeding in lower vertebrates. In: Hildebrand, M., et al., (Eds.),
755 *Functional Vertebrate Morphology*. Harvard Univ Press, Cambridge, MA, pp. 185-229.

756 Liem, K. F., 1967. Functional morphology of the head of the anabantoid teleost fish *Helostoma*
757 *temmincki*. J Morphol 121, 135-157.

758 Liem, K. F., 1978. Modulatory multiplicity in the functional repertoire of the feeding mechanism
759 in cichlid fishes. I. Piscivores. J Morphol 158, 323-360, doi:10.1002/jmor.1051580305.

760 Liem, K. F., 1980. Acquisition of energy by teleosts: adaptive mechanisms and evolutionary
761 patterns. In: Ali, M. A., (Ed.), Environmental Physiology of Fishes. Plenum Publishing
762 Corporation, New York, NY, pp. 299-334.

763 Marsh, R., Olson, J., Guzik, S., 1992. Mechanical performance of scallop adductor muscle
764 during swimming. Nature 357, 411-413.

765 Mendez, J., Keys, A., 1960. Density and Composition of Mammalian Muscle. Metabolism 9,
766 184-188.

767 Muller, M., Osse, J., Verhagen, J., 1982. A quantitative hydrodynamical model of suction
768 feeding in fish. J Theor Biol 95, 49-79.

769 Near, T. J., Bolnick, D. I., Wainwright, P. C., 2004. Investigating phylogenetic relationships of
770 sunfishes and black basses (Actinopterygii: Centrarchidae) using DNA sequences from
771 mitochondrial and nuclear genes. Mol Phylogen Evol 32, 344-357.

772 Norton, S. F., Brainerd, E. L., 1993. Convergence in the feeding mechanics of
773 ecomorphologically similar species in the Centrarchidae and Cichlidae. J Exp Biol 176,
774 11-29.

775 Peplowski, M. M., Marsh, R. L., 1997. Work and power output in the hindlimb muscles of cuban
776 tree frogs *Osteopilus septentrionalis* during jumping. J Exp Biol 200, 2861-2870.

777 Rome, L. C., Sosnicki, A. A., 1991. Myofilament overlap in swimming carp. II. Sarcomere
778 length changes during swimming. Am J Physiol 260, C289-96.

779 Rome, L. C., Funke, R. P., Alexander, R. M., Lutz, G., Aldridge, H., Scott, F., Freadman, M.,
780 1988. Why animals have different muscle fibre types. Nature 335, 824-827.

781 Shadwick, R. E., Steffensen, J. F., Katz, S. L., Knowler, T., 1998. Muscle dynamics in fish during
782 steady swimming. Am Zool 38, 755-770.

783 Smith, A. J., Nelson-Maney, N., Parsons, K. J., James Cooper, W., Craig Albertson, R., 2015.
784 Body Shape Evolution in Sunfishes: Divergent Paths to Accelerated Rates of Speciation
785 in the Centrarchidae. Evolutionary Biology 42, 283-295, doi:10.1007/s11692-015-9322-
786 y.

787 Van Wassenbergh, S., 2015. A Solution Strategy to Include the Opening of the Opercular Slits in
788 Moving-Mesh CFD Models of Suction Feeding. Integr Comp Biol 55, 62-73,
789 doi:10.1093/icb/icv031.

790 Van Wassenbergh, S., Dries, B., Herrel, A., 2014. New Insights into Muscle Function during
791 Pivot Feeding in Seahorses. PLoS ONE 9, e109068, doi:10.1371/journal.pone.0109068.

792 Van Wassenbergh, S., Herrel, A., Adriaens, D., Aerts, P., 2005. A test of mouth-opening and
793 hyoid-depression mechanisms during prey capture in a catfish using high-speed
794 cineradiography. J Exp Biol 208, 4627-39, doi:10.1242/jeb.01919.

795 Van Wassenbergh, S., Herrel, A., Adriaens, D., Aerts, P., 2007a. Interspecific variation in
796 sternohyoideus muscle morphology in clariid catfishes: Functional implications for
797 suction feeding. Journal of Morphology 268, 232-242, doi:10.1002/jmor.10510.

798 Van Wassenbergh, S., Herrel, A., Adriaens, D., Aerts, P., 2007b. Interspecific variation in
799 sternohyoideus muscle morphology in clariid catfishes: functional implications for
800 suction feeding. J Morphol 268, 232-42, doi:10.1002/jmor.10510.

801 Van Wassenbergh, S., Strother, J., Flammang, B., Ferry-Graham, L., Aerts, P., 2008. Extremely
802 fast prey capture in pipefish is powered by elastic recoil. *J R Soc Interface* 5, 285-296,
803 doi:10.1098/rsif.2007.1124.

804 Van Wassenbergh, S., Day, S. W., Hernández, L. P., Higham, T. E., Skorczewski, T., 2015.
805 Suction power output and the inertial cost of rotating the neurocranium to generate
806 suction in fish. *J Theor Biol* 372, 159-167, doi:10.1016/j.jtbi.2015.03.001.

807 Van Wassenbergh, S., Lieben, T., Herrel, A., Huysentruyt, F., Geerinckx, T., Adriaens, D.,
808 Aerts, P., 2009a. Kinematics of benthic suction feeding in Callichthyidae and
809 Mochokidae, with functional implications for the evolution of food scraping in catfishes.
810 *The Journal of Experimental Biology* 212, 116-25.

811 Van Wassenbergh, S., Roos, G., Genbrugge, A., Leysen, H., Aerts, P., Adriaens, D., Herrel, A.,
812 2009b. Suction is kid's play: extremely fast suction in newborn seahorses. *Biol Lett* 5,
813 200-3, doi:10.1098/rsbl.2008.0765.

814 Wainwright, P. C., McGee, M. D., Longo, S. J., Hernandez, L. P., 2015. Origins, Innovations,
815 and Diversification of Suction Feeding in Vertebrates. *Integrative and Comparative*
816 *Biology* 55, 134-145, doi:10.1093/icb/icv026.

817 Werner, E. E., 1977. Species Packing and Niche Complementarity in Three Sunfishes. *The*
818 *American Naturalist* 111, 553-578.

819 Westneat, M. W., 2006. Skull Biomechanics and Suction Feeding in Fishes. In: Shadwick, R. E.,
820 Lauder, G., Eds.), *Fish Physiology*. Academic Press, San Diego, CA, pp. 29-75.
821
822

823 **Tables**

824

825 **Table 1.** Mean (s.e.m) timing and magnitude of peak muscle strain (% initial length (L_i), positive
 826 values indicate shortening), velocity during the period of peak power (positive values indicate
 827 shortening) and bilateral muscle mass for each individual.

Muscle	Variable	Bluegill 1 ($N = 6$)	Bluegill 3 ($N = 5$)
Epaxials	Strain (%)	3.9 (0.5)	4.4 (0.9)
	Time ^a of peak strain (ms)	4.3 (1.5)	10.8 (2.2)
	Velocity ($L_i s^{-1}$)	2.2 (0.3)	1.9 (0.5)
	Mass (g)	26.4	26.2
Hypaxials	Strain (%)	6.8 (0.6)	5.5 (0.9)
	Time ^a of peak strain (ms)	8.7 (2.0)	12.0 (6.1)
	Velocity ($L_i s^{-1}$)	3.4 (0.2)	2.1 (0.6)
	Mass (g)	14.8	13.1
Levator Arcus Palatini	Strain (%)	10.1 (0.9)	5.7 (1.2)
	Time ^a of peak strain (ms)	39.7 (7.1)	39.6 (5.0)
	Velocity ($L_i s^{-1}$)	1.4 (0.7)	-0.45 (0.5)
	Mass (g)	0.20	0.22
Dilator Operculi	Strain (%)	8.5 (1.1)	10.6 (2.2)
	Time ^a of peak strain (ms)	41.3 (6.5)	44.0 (4.3)
	Velocity ($L_i s^{-1}$)	2.1 (0.8)	-1.9 (1.1)
	Mass (g)	0.10	0.10
Levator Operculi	Strain (%)	6.9 (1.1)	7.3 (0.9)
	Time ^a of peak strain (ms)	10.3 (1.8)	7.6 (2.3)
	Velocity ($L_i s^{-1}$)	3.2 (1.0)	3.3 (0.6)
	Mass (g)	0.06	0.10
Sternohyoideus	Strain (%)	12.0 (1.0)	4.4 (1.2)
	Time ^a of peak strain (ms)	11.3 (1.3)	-3.6 (12.7)
	Velocity ($L_i s^{-1}$)	4.4 (0.5)	1.4 (0.7)
	Mass (g)	1.5	2.4

^aTime relative to the time of peak gape

828

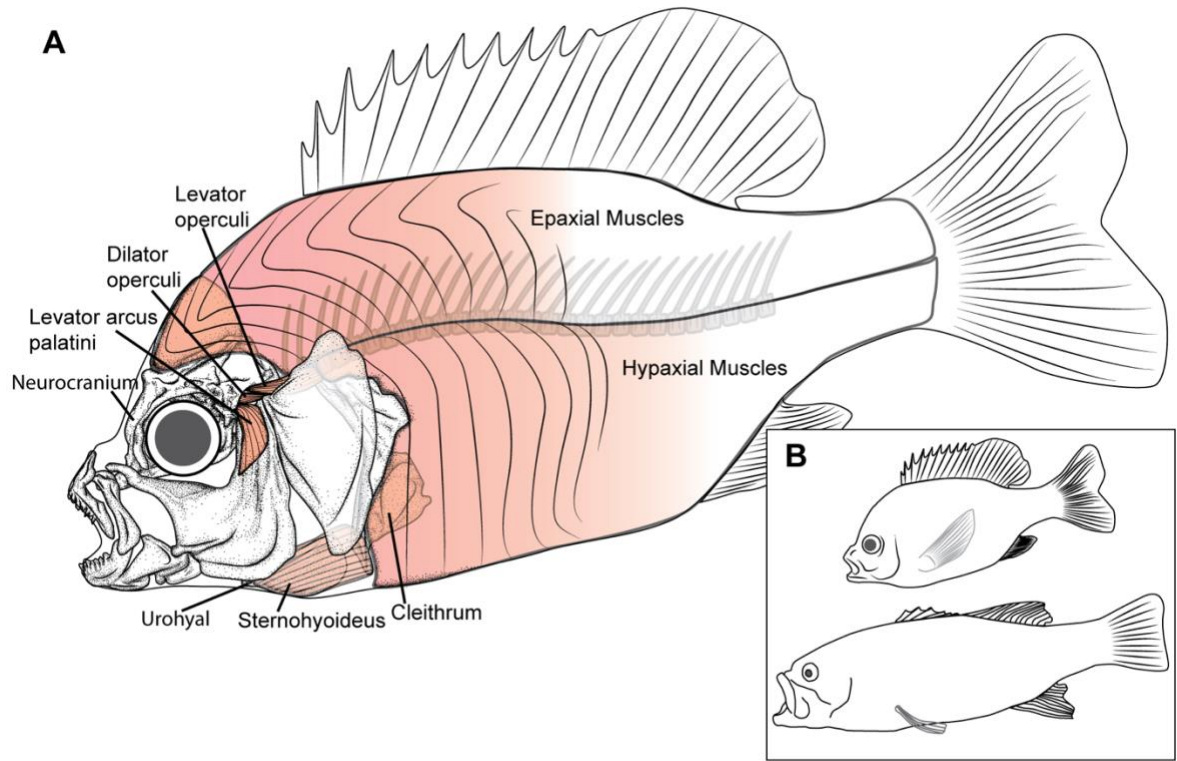
829 **Table 2.** Mean (s.e.m) timing and magnitude of peak pressure, volume, power, and work of
 830 suction feeding strikes, along with body and summed, bilateral muscle masses.

Variable		Bluegill 1 (<i>N</i> = 6)	Bluegill 3 (<i>N</i> = 5)
Pressure	Pressure (kPa)	-32.2 (2.2)	-17.2 (4.6)
	Time ^a of min. pressure (ms)	-1.7 (2.3)	-10.8 (1.9)
Volume	Volume (cm ³)	18.3 (1.0)	18.4 (1.0)
	Time ^a of peak volume (ms)	12.7 (1.6)	14.4 (2.7)
	Volume rate (cm ³ s ⁻¹)	386.5 (58.2)	351.2 (74.9)
	Time ^a of peak volume rate (ms)	-5.3 (2.6)	-5.2 (2.2)
Power	Power (W)	11.4 (2.1)	5.2 (2.1)
	Time ^a of peak power (ms)	-4.3 (2.6)	-9.2 (1.4)
Work	Work (J)	0.14 (0.03)	0.07 (0.02)
Mass	Total body (g)	164	162
	All cranial muscles (g)	1.86	2.84
	All axial muscles (g)	41.1	39.12

^aTime relative to time of peak gape

831

832 **Figures**

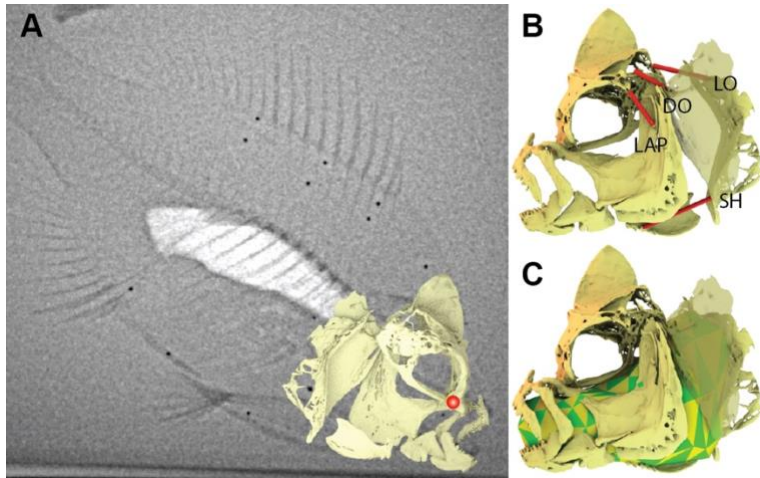


833

834 **Figure 1. Muscles of the feeding apparatus and the muscles of suction expansion in the**
835 **bluegill sunfish. (A)**The regions of the axial muscles that consistently shortened during suction
836 feeding are colored solid red, with decreasing color intensity indicating generally decreasing
837 shortening until ultimately regions without shortening are colorless (white). **(B)** Whole body
838 shape of bluegill sunfish and largemouth bass.

839

840

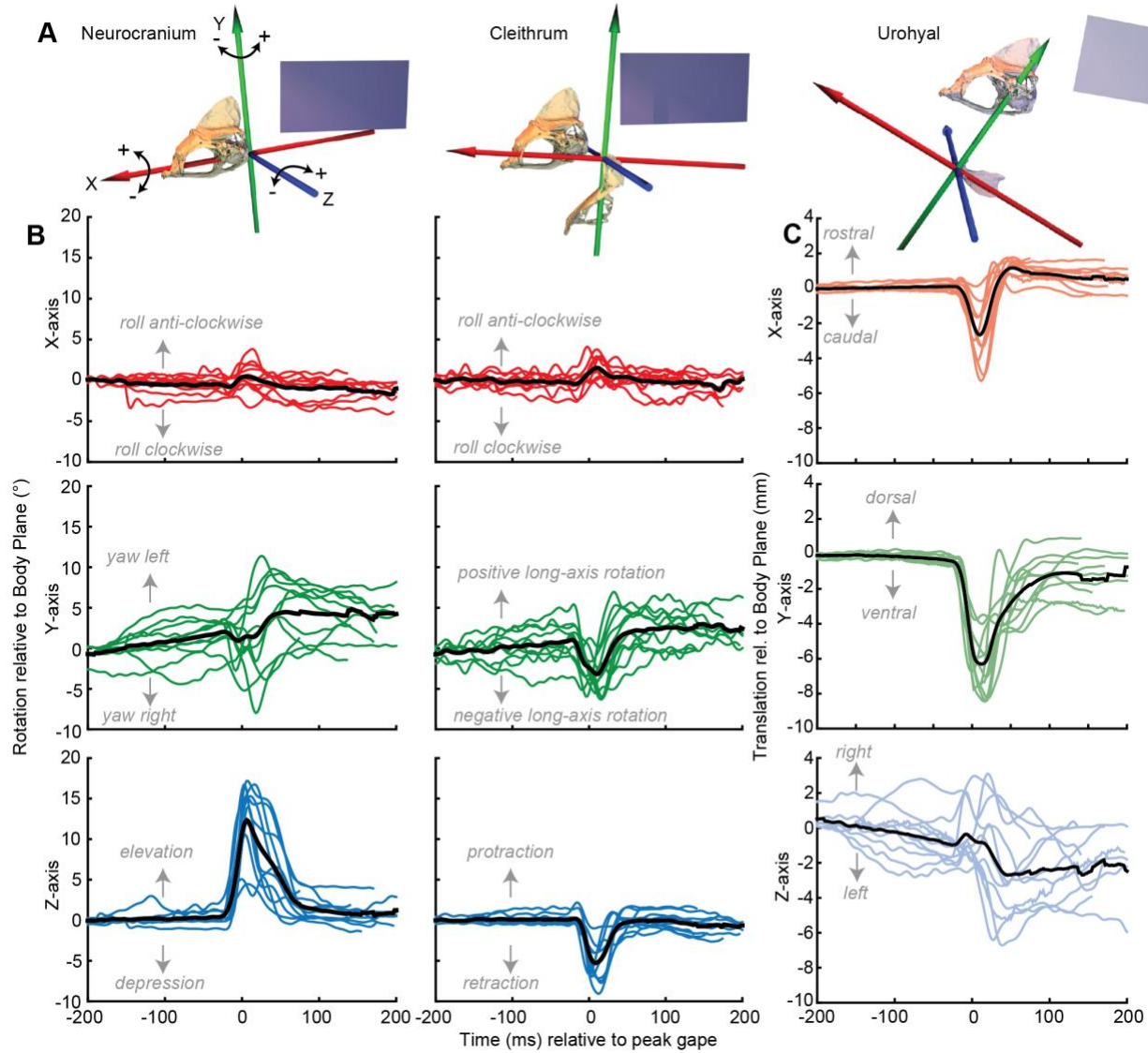


841

842 **Figure 2. Sample XROMM animation and measurements of suction expansion.** (A) Right
843 medial-view X-ray image with animated bone models superimposed (neurocranium, urohyal and
844 left-side bones only). Intramuscular markers for fluoromicrometry and the body plane are visible
845 along the dorsal and ventral edge of the epaxial and hypaxial muscles, respectively. The location
846 of the pressure transducer is indicated by the red sphere. Left lateral view of animated bone
847 models with (B) muscle length measurements (red lines) of the levator arcus palatini (LAP),
848 dilator operculi (DO), levator operculi (LO) and sternohyoideus (SH) muscles, and (C) the
849 dynamic digital endocast (green and yellow) used to measure volume.

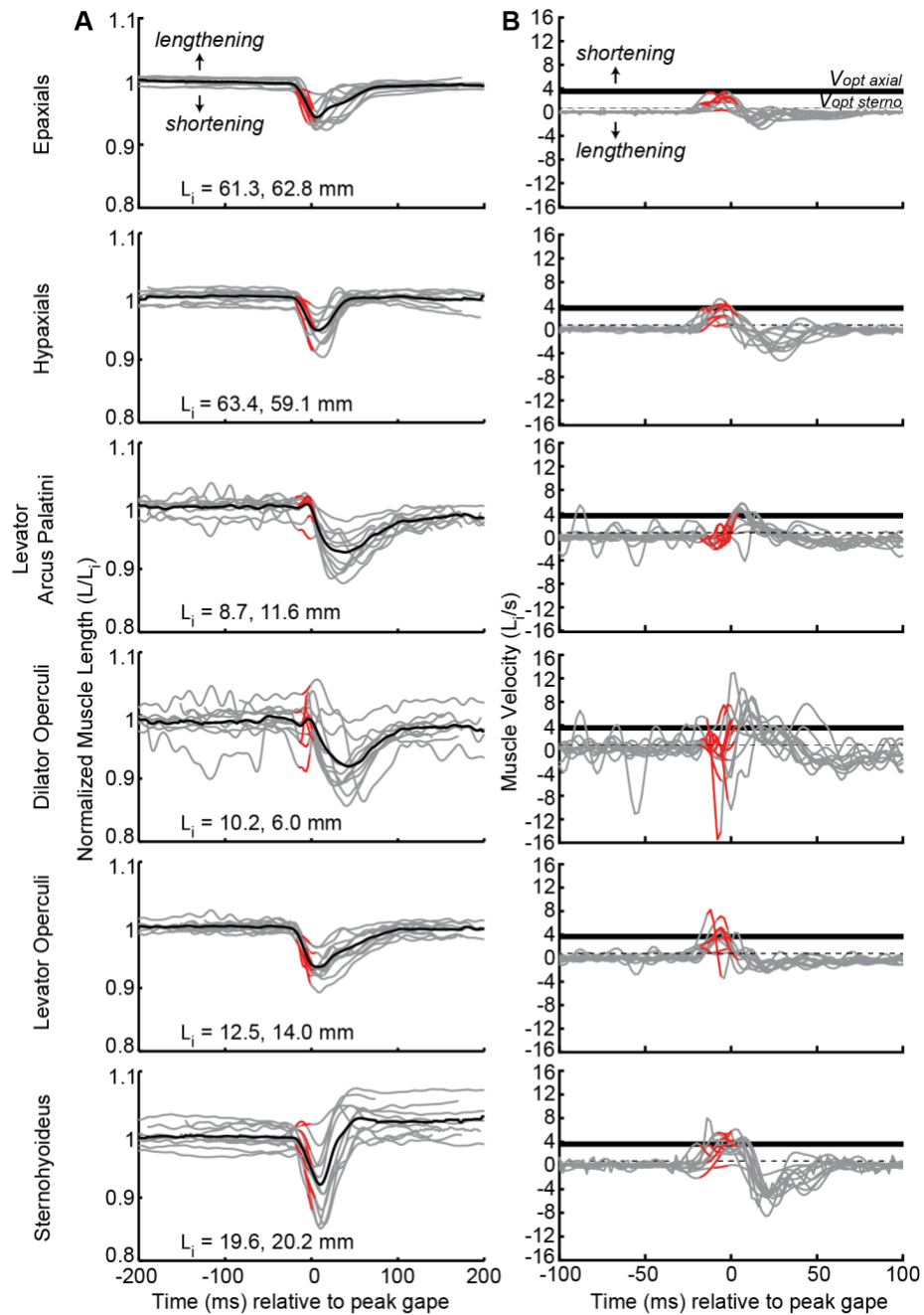
850

851



852

853 **Figure 3. Rotations of the neurocranium and cleithrum and translations of the urohyal,**
 854 **relative to the body plane.** (A) For each bone, rotations were measured about each axis of the
 855 joint coordinate systems. Euler angles were calculated with a ZYX rotation order, with polarity
 856 determined by the right-hand rule with thumb pointed toward the arrow head for each axis. Bone
 857 models (in yellow) are shown along with the body plane (blue rectangle). Rotations (B) or
 858 translations (C) are shown from each strike (thin colored lines), as well as the mean rotation or
 859 translation (thick black lines) at each time step. Clockwise roll of the neurocranium and
 860 cleithrum are defined from a frontal view, and negative long-axis rotation of the cleithrum is
 861 clockwise in dorsal view. Means are calculated across both individuals and all strikes ($N = 11$
 862 strikes).



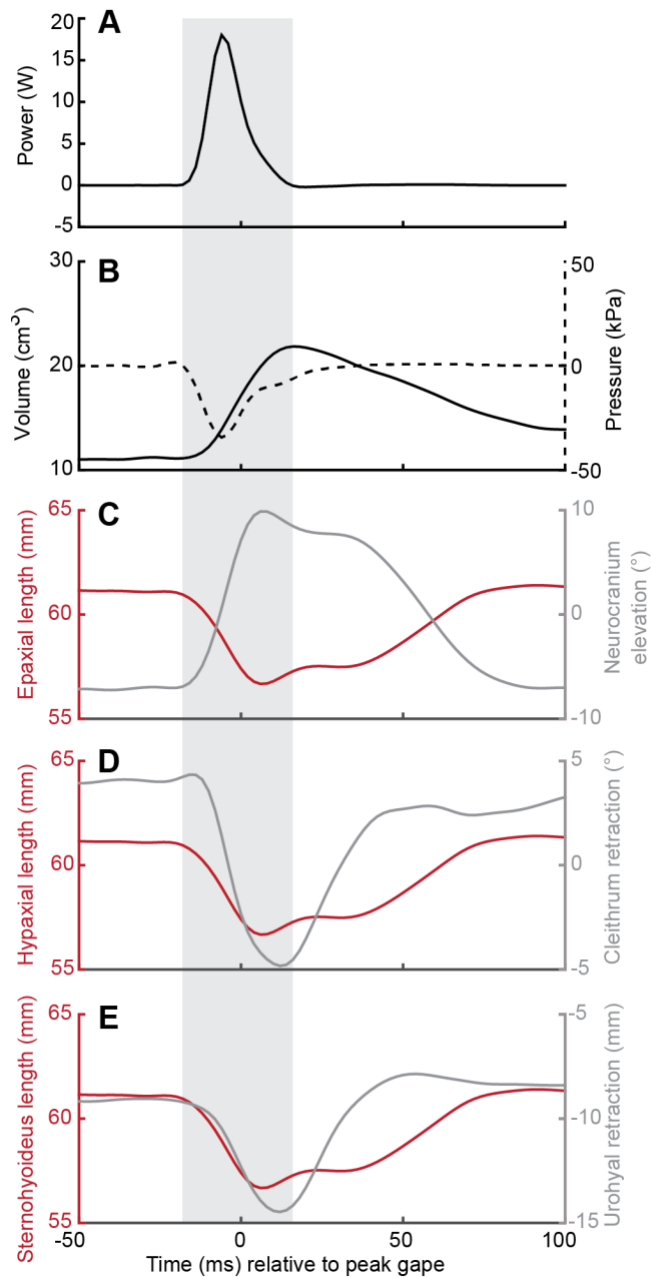
863

864 **Figure 4. Normalized muscle length and velocity during suction feeding.** For both panels,
 865 traces from individual strikes (grey lines) are shown with the values during peak (within 25% of
 866 maximum) expansion power highlighted (red lines). **(A)** Length of each muscle normalized to its
 867 mean initial muscle length (L_i), with L_i values listed for Bluegill 1 and Bluegill 3, respectively.
 868 Decreasing values indicate shortening. The mean length at each time point (across all strikes and
 869 both individuals, $N = 11$ strikes) is also shown for each muscle (black lines). **(B)** Instantaneous

870 velocity of each muscle, with the optimum velocity for power production of the sternohyoideus
871 ($V_{opt\ sterno}$, dashed line) and the axial muscles ($V_{opt\ axial}$, solid bar), which spans the V_{opt} measured
872 for epaxial and “myotomal” muscles (Carroll et al., 2009). Note that for velocity, positive values
873 indicate shortening.

874

875



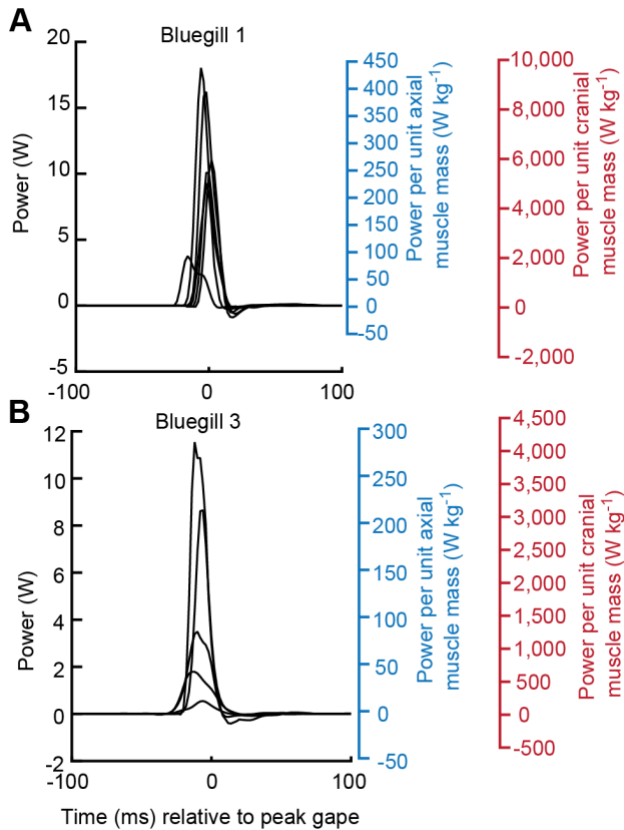
876

877 **Figure 5: Expansion power, muscle length, and skeletal kinematics from the most powerful**
 878 **sunfish strike recorded (Bluegill 1).** Power (A) is estimated from the product of buccal pressure
 879 (B) and rate of bilateral mouth volume change (note that absolute volume is shown in B). Whole-
 880 muscle lengths of the epaxial (C), hypaxial (D), and sternohyoideus (E) are shown in mm, and
 881 not relative to initial lengths. Neurocranium elevation (C) cleithrum retraction (D), and urohyal
 882 retraction (E) are measured relative to the body plane, and again magnitudes are not relative to
 883 initial values. The grey bar indicates the period of power production. Note that the onset of

884 muscle shortening and corresponding skeletal motion are generally coincident, indicating an
885 absence of muscle shortening prior to power production.

886

887



888

889 **Figure 6. Suction expansion power for each strike from (A) Bluegill 1 and (B) Bluegill 3.**

890 The absolute magnitude of power (W) estimated for expansion is shown in black on the left Y-

891 axis, graphed as a function of time. The two right Y-axes express these same power magnitudes

892 as mass-specific power (W kg^{-1}) by dividing the estimated expansion power by the total mass of

893 the axial muscles (blue axis) or by the total mass of the four cranial muscles (red axis) of each

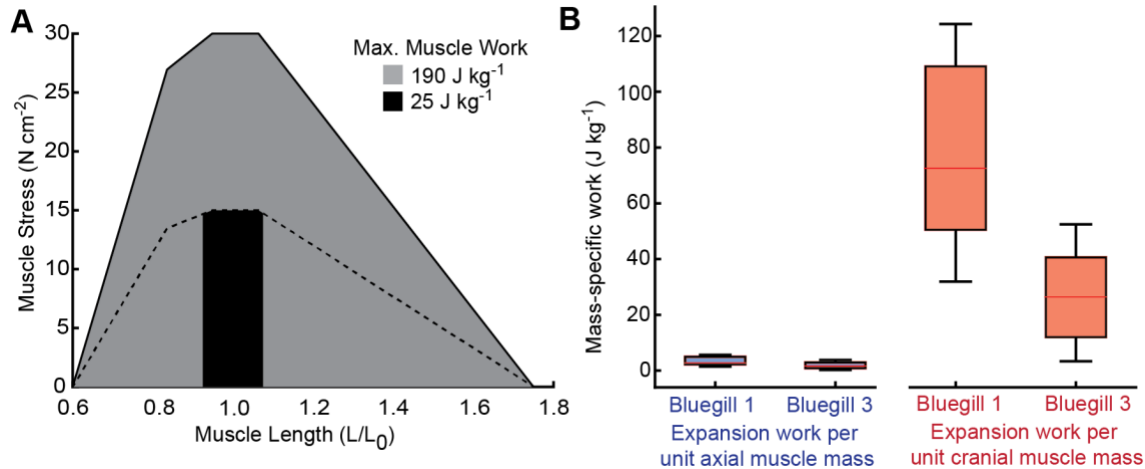
894 individual. These mass-specific powers represent the estimated power outputs the axial or cranial

895 muscles would have to generate, assuming they were the sole source of power for suction

896 expansion.

897

898

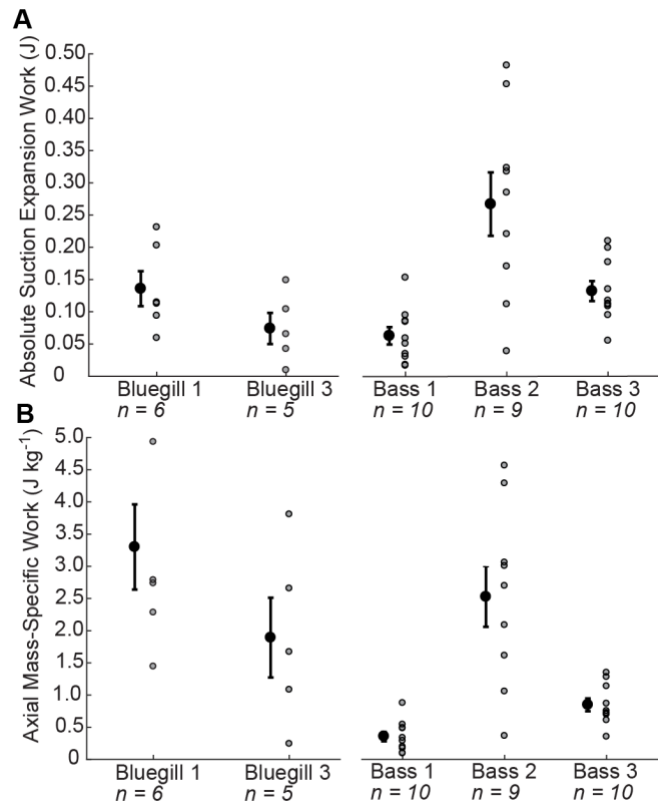


899

900 **Figure 7. Estimated muscle work capacity and mass-specific work of expansion during**
 901 **sunfish suction feeding.** (A) Vertebrate muscle length tension curve (redrawn from Peplowski
 902 and Marsh, 1997 and assuming a maximum isometric force of 30 N cm⁻²). Theoretical work
 903 capacity (J kg⁻¹) of the muscle was calculated as the area under the curve, divided by the density
 904 of vertebrate muscle (1.06 x 10⁹ kg cm⁻³ (Mendez and Keys, 1960)), and finally divided by 100
 905 to convert from N cm kg⁻¹ to N m kg⁻¹ so that the final value is in J kg⁻¹. Assuming the muscle
 906 shortens infinitely slowly and with 115% strain, i.e., from 175% of its optimal length (L_o) to 60%
 907 of its optimal length, it could produce 190 J kg⁻¹ of work (grey shaded area). A more realistic
 908 estimate of maximum work capacity is shown by the black shaded region (25 J kg⁻¹), which
 909 assumes only a 15% strain (based on *in vivo* shortening measured in this study) and that the rapid
 910 muscle shortening required for powerful feeding will result in a 50% reduction in force due to
 911 force-velocity effects (Peplowski and Marsh, 1997). (B) The estimated mass-specific work of
 912 suction expansion, calculated as the area under the power-time curve for each strike, divided by
 913 the mass of the axial muscles (blue, left-side boxplots) or by the mass of the cranial muscles (red,
 914 right-side boxplots). Each boxplot shows the mean (red line), the 25-75% percentile (box edges),
 915 and extreme values (whiskers) of mass-specific work required for each individual (*N* = 6 strikes
 916 for Bluegill 1, *N* = 5 strikes for Bluegill 3), assuming only the axial (left hand bars) or cranial
 917 (right hand bars) muscles produce the work of suction.

918

919



920

921 **Figure 8: Estimated expansion work in bluegill sunfish (from this study) and largemouth**

922 **bass (data from Camp et al., 2015). (A) Absolute magnitude of suction expansion work during**

923 **feeding strikes. (B) The same suction expansion work, expressed per unit axial muscle mass, i.e.,**

924 **the summed mass of the hypaxial and epaxial muscles. In both panels, for each individual the**

925 **expansion work is shown for each strike (grey filled circles) along with the mean expansion**

926 **work (filled black circle) and standard error (black lines) for that individual. The number of**

927 **strikes, from which means and standard errors were calculated, are listed beneath each**

928 **individual. Bluegill mean axial mass-specific work is the same as that shown in Fig. 7, but**

929 **included here for comparison with largemouth bass.**

930